Efficient hexapodal locomotion control based on flow-invariant subspaces

E. Arena, P. Arena, L. Patanè

Dipartimento di Ingegneria Elettrica Elettronica e Informatica, University of Catania, Catania, Italy, (e-mail:parena@dieei.unict.it)

Abstract: In this paper the issue of locomotion control in bio-inspired hexapod structures is considered as a problem of convergence toward flow invariant subspaces in networks of mutually and locally coupled neural units. Since the network topologies used refer to undirected diffusive tree graphs, in this case a unique gain value on the graph connection matrix can be found to guarantee exponential convergence to any desired gait (i.e. phase locked) configuration. Such sufficient condition is exploited for the locomotion control in a hexapod structure. In the paper, after dealing with the sufficient condition above mentioned, both simulation and experimental results on a robotic hexapod structure are reported. Moreover the role of key parameters for insect inspired turning strategies is investigated.

1. INTRODUCTION

Most animals walk in a stereotyped way, adopting rhythmic motion patterns. In a large variety of animals (Orlovsky *et al*., 1999)), the neural control of locomotion is hierarchically organized. The key point is the presence of a functional unit, called the *Central Pattern Generator* (CPG), containing the key mechanisms needed to generate the rhythmic motion patterns. It essentially provides the feedforward signals needed for locomotion, even in the absence of sensory feedback, and high-level control. Examples of successful applications of the CPG are the biomimetic walking robots (Klaassen *et al*., 2002), underwater robots, hexapod robots (Zielinska *et al*., 1998) (Quinn *et al*., 1998), quadrupeds (Fukuoka *et al*., 2003) and bipeds (Lewis *et al*., 2002). Several works were inspired by seminal works on bio-inspired approaches, like. (Beer *et al*., 1992). As in (Collins *et al*., 1993) (Golubtisky *et al*., 1998) CPGs are viewed as networks of coupled nonlinear systems with given connections and parameters to be modulated in order to account for distinct gaits. The control of the overall structure is conceived as the task of assigning, in steady state conditions, a well defined phase shift among the cells composing the CPG architecture, so that the network reaches a *phase-shift synchronization* regime (Seo *et al*., 2007). The emerging solution is a travelling wave pattern which visits all the motor neurons and thus imposes a specific gait to the controlled robotic structure. The authors have been involved in the design of CPGs and in their realization by means of locally coupled Cellular Neural Networks (Frasca *et al*., 2004), going down into the implementation issue with VLSI CPG analog networks on chip (Arena *et al*., 2005). The research already done is being now revisited in light of modern stability analysis on steady state trajectories for non linear systems based on contraction theory introduced in (Lohmiller *et al*., 1996), and later on extended to Partial Contraction (Wang *et al*., 2005) to include exponential convergence to behaviours or even to specific relations among the state variables, instead of trajectories. This approach was extended (Pham *et al*., 2007) and applied in (Seo *et al*., 2007) to generate models for CPG-based locomotion. These manuscripts referred to general graphs networks, including single chain models as well as networks possessing internal loops. Sufficient powerful conditions for global exponential convergence to flow-invariant subspaces were introduced, linking the algebraic connectivity of the underlying graph network to the eigenvalues of the dynamics embedded into each single neuron. In this paper such analysis is taken into account and particularised to the case of tree graphs. This is the case of most CPG networks. Here a simple analysis leads to enlarge the efficacy of the sufficient conditions above, with the derivation of a unique gain value that does not depend on the particular subspace imposed. In the paper this property is exploited and applied to the locomotion control issue for a hexapod structure, which will exhibit a number of different locomotion gaits, ranging from the slow to the medium to the fast gait, even in a continuous way, as some insect species show. Moreover, the strategy is suitable for hosting a feedback control for typical steering patterns met in insects. Starting once again from the results reported in (Seo., 2007), we also apply a feedback law that modulates the frequency of a reduced number of oscillators in the network. We exploit the effect of a frequency modulation in terms of phase and amplitude variation in the overall network to obtain efficient steering patterns which strictly resemble those ones described in insects. All the results proposed are tested on a dynamic simulation environment, and in some cases also on a hexapod robot prototype: the Minihex. This is controlled by a custom board built around a digital low cost microcontroller, however, the same strategy can be applied to an analog, digitally programmable VLSI chip, already available in our laboratory (Arena *et al*., 2005).

2. CPG IN HEXAPODS, STABILITY AND CONTRACTION ANALYSIS

The results on partial contraction theory are applied to a network of CPG cells for locomotion control in a hexapod-like topology. In the following, the equations characterizing each basic unit and the proprieties of the connection matrix leading to a global exponentially converging phase locked synchronization will be discussed, referring to a tree-graph

network topology. Even if the analysis will deal with a particular cell dynamics, usually employed in our CPG-based structure, the discussion could be extended to general smooth nonlinear oscillators embedded into undirected diffusive tree graphs. So the following notation will be used:
n_n: number of neurons in the network;
n_c: order of the single neuron;
$n_t = n_n \times n_c$: total number of state variables in the network.

2.1 CPG cell model and connection definition

The basic elements of the dynamical network are second-order cells, each one described by the equations below:

$$\begin{cases} x_{1,i} = -x_{1,i} + (i + \mu + \varepsilon) y_{1,i} - s_1 y_{2,i} + i_1 \\ x_{2,i} = -x_{2,i} + s_2 y_{1,i} + (i + \mu - \varepsilon) y_{2,i} + i_2 \end{cases} \quad (1)$$

with $y_i = \tanh(x_i)$. The parameters used to allow each cell oscillate with a stable *limit cycle*, are: $\mu = 0.7$, $\varepsilon = 0$, $s_1 = s_2 = s = 1$, $i_1 = 0$, $i_2 = 0$ (Frasca *et al*., 2004).
The dynamical network is thus built up connecting n_n identical cells in the following way (Seo *et al*., 2007):

$$x_i = f(x_i, t) + k \sum_{j \neq i;\, j \in N_\eta} (R_{ij} x_j - x_i) \quad \text{with} \quad i, j = 1,...n_n \quad (2)$$

where the summation is extended to all the neurons j belonging the neighborhood of radius one for the neuron i, i.e. to all the immediately adjacent neurons for neuron i; $f(x_i,t)$ represents the intrinsic dynamic of the i-th uncoupled oscillator, k is a parameter determining the "strength" of the connections and the sum of terms is given by the *diffusive* couplings between the i-th and j-th node. In the case treated in the paper, being the system in eq.(1) a second order dynamics, it results that $n_c = 2$ and so the term R_{ij} in eq.(2) represents the desired phase shift between the two oscillators, described through a rotation matrix in R^2. We assume that the connections are bidirectional and such that $R_{ij} = R_{ji}^T$ in order to have a balanced and undirected network. Moreover, in eq. (2) the concept of diffusive coupling refers to a direct dependence of the connection value on the difference between the two connected oscillators states. In the traditional definition, the diffusion effect vanishes when the two oscillators are in the same state. Here the concept includes conditions in which the diffusive effect has to vanish in presence of a desired phase shift specified by the rotation matrix R_{ij} in eq.(2). The dynamics of the whole system performing the phase-shift synchronization can be written as:

$$\dot{x} = f(x) - k \cdot L \cdot x \quad (3)$$

where x is the state variables vector ($x_{1,...,}\ x_{nr}$), $f(x)$ is the vector of the state functions $f(x_i)$, associated to the x vector, $(f(x_{1),...,}\ f(x_{nr}))^T$, and L is the coupling matrix built up blocks $L_{ij} \in \Re^{n_c \times n_c}$. Since we are focused upon undirected and balanced tree networks, each L_{ij} block is defined through the following relations:

1. $L_{ij} = -R(\phi_{ij})$ if the i-th node diffuses to the adjacent j-th node, locking its state dynamics to phase lock of ϕ_{ij}.
2. $L_{ji} = -R(-\phi_{ji})$ if $L_{ij} = -R(\phi_{ij})$ to satisfy the phase periodicity conditions between nodes i and j in an undirected graph.
3. $L_{ij} = L_{ji} = 0$ if no direct connection joins nodes i and j.
4. $L_{ii} = d_i \cdot I_{nc}\ \forall\ i = 1..n_n$, where d_i is the unweighted degree of the i-th node.

Then, for sake of simplicity, supposing to consider a system with chain-topology like that one shown in Fig.1:

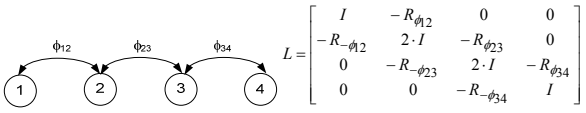

a) b)

Fig. 1. a) a general chain topology; b) the corresponding connection matrix L

Let us assume that all nodes are completely synchronized, with a null phase shift among them, and let us call L_0 the connection matrix. L_0 corresponds to the traditional zero-row sum Laplacian matrix associated to the graph, which, as well known, is symmetric and positive semi-definite.
In case of arbitrary phase rotations among the oscillators, it has to be considered that, since from eq. (2) it results $R(-\phi) = R(\phi)^T$, the L matrix is still block symmetric. Moreover it results to be similar to the matrix L_0, as it can be directly proven using the following nonsingular transformation matrix: $T = diag[R(0)\ \ R(\phi_{12})\ \ R(\phi_{12}) \cdot R(\phi_{23}) ..]$.
As it will be discussed in next Section, the so defined dynamics equation (3) and the chosen structure for the matrix L are suitable in order to directly apply results from Partial Contraction theory (Wang *et al*., 2005).

2.2 Partial Contraction analysis in a tree graph CPG-CNN

The methodology adopted in the following is clearly presented in (Pham. *et al*., 2007): it is inspired by the partial contraction analysis for nonlinear systems. It starts from the definition of a flow-invariant subspace M, in which the system trajectories are desired to be trapped, and in the construction of its orthogonal complement V, in which the dynamics of an auxiliary virtual system has to be contractive. The M subspace is determined by the rotational constraints which impose prescribed phase shifts among the cells. In general, M is constituted by p vectors, each one representing the desired phase-shifts among the neurons belonging to each of the p different groups of nodes. Then, for the network in eq.(3), the generic block M_r is: $Mr = \{L_{ij}\ xj = x_i\ \ \forall\ i \neq j\} \in R_{nt,nc}$, with r = 1,..,p and the global M subspace is given by the p rectangular matrices $(M_1, M_2, \ldots M_p)$. M is a $n_t \times (p \times n_c)$ block matrix. Consequently, the orthonormal complement V of the flow invariant subspace M, on which the components of the trajectories of the auxiliary system have to contract, is the $n_t \times (n_t - (p \times n_c))$ block matrix having as columns: $(Mp+1^T, \ldots, Mnn^T)$. Of course it results: $x \in M \Leftrightarrow Vx = 0$.

Notably, the construction and the dimensions of M strictly depend on the network topology. If the nodes are connected as a generic tree-like structure, the phase locking constraints can be exhaustively imposed through one single M_r rectangular matrix, where each block describes the desired phase shift with respect to a reference node. When the topology shows multiple paths to reach a given node, for example in presence of loops, two or more synchronization groups have to be defined to lock the phase along all

directions, having thus r>1. So, in our case, taking into account specifically the chain in Fig. 1, let the first node be the reference one, then the M subspace is defined as follows:

$$M = \left(\left[\mathrm{R}_0{}^T \quad \mathrm{R}_{\phi_{12}}{}^T \quad (\mathrm{R}_{\phi_{12}} \cdot \mathrm{R}_{\phi_{23}})^T \quad (\mathrm{R}_{\phi_{12}} \cdot \mathrm{R}_{\phi_{23}} \cdot \mathrm{R}_{\phi_{34}})^T \right] \right)^T$$

Since r=1, $M \in \mathrm{R}^{n_t \times n_c}$ and $V \in \mathrm{R}^{n_t \times (n_t - n_c)}$.

The projection of the connection matrix L into the orthogonal subspace defines the bounds where the convergence to the flow invariant manifold is assured in relation with the intrinsic properties of each single cell.

According to (Wang *et al.*, 2005), if the network is balanced, undirected[1] and the coupling matrix is positive semidefinite, as in the case of Fig.1, the sufficient condition (4) gives us a constraint on the minimum value of k that assures the global phase locked synchronization within M.

$$k \cdot \lambda_{\min}(V^T L V) > \sup_{x_i,t} \lambda_{\max}\left(\frac{\partial f}{\partial x}(x_i, t) \right) \qquad (4)$$

This relation describes how much the coupling forces need to be "strong" in order to dominate the Jacobian dynamics of the uncoupled system and thus perform the desired phase-locked synchronization. A simple but useful result can be derived dealing with tree graphs, like our case. This result allows to guarantee the exponential convergence to any locomotion gait on the basis of one a-priori fixed value of k.

3. CPG GENERATION AND CONTROL IN HEXAPODS

As previously recalled, a particular locomotor program consists of a series of signals with a well defined phase shift. The various phase delays among the cells representing particular robot joints are obtained imposing particular rotation shifts among the state variables of the corresponding oscillators having the dynamics reported in eq.(1).

After the main results reported in (Pham. *et al.*, 2007), the choice of considering tree structures derives from algebraic inspection on the invariant proprieties of graphs. In fact, it can be shown (see Appendix) that connectivity matrices on graphs having the same topology (vertex number, edges and connection direction) preserve similarity under arbitrary phase shifts in the corresponding i-th rotational blocks. Given the particular tree and connection structure, rotations affect only off-diagonal blocks (Fig.1). Therefore the connection matrices possess the same diagonal blocks, which depend only on the unweighted degree of the i-th node. Thus we can derive the following:

For the system in eq.(3), defined on a given tree graph, let us consider a flow-invariant subspace M, defining an arbitrarily chosen locomotion pattern (i.e. a phase shift among the oscillators), and let us consider the associated orthonormal complement V. Solutions of system (3) converge exponentially to M if it holds:

$$k \cdot \lambda_1 > \sup_{x_i,t} \lambda_{\max}\left(\frac{\partial f}{\partial x}(x_i, t) \right) \qquad (5)$$

where $\lambda_1 = \lambda_{\min}(V^T L V) = \lambda_{\min}(L)$

λ_1 is defined as the algebraic connectivity of the graph according to Fiedler's theory (Fiedler et al., 1973).

The result stated above gives us a sufficient condition on the minimum *k* value that guarantees global exponential convergence to any chosen locomotion gait. This value can be a priori determined by simply knowing the algebraic connectivity of the tree-graph and the maximum value, along the uncoupled system trajectory, of its largest Jacobian eigenvalue. Thanks to the invariant properties the L matrix, once defined this value for *k*, we can start with any desired locomotion gait, then switch the connection matrix from one gait to any other desired one, having assured exponential convergence of the system trajectories to the new imposed phase-locked configuration. Below a series of simulations and some multimedia experimental results on our robot prototype are reported.

4. SIMULATION AND EXPERIMENTAL RESULTS

From the above results, the condition on the k parameter depends on the ratio between the maximum Jacobian eigenvalue for the uncoupled system and the graph algebraic connectivity. This result leads to important consequences on the global control of any CPG gait within the same neural topology.

In order to perform the locomotion control of our hexapod, the tree graph network in Fig 2 has been taken in account. Stable limit cycle for each neuron is reached using Eq.(1), whereas the L matrix is built according to the four rules outlined in Section 2.1. The model, in fact, represents an extension of the chain in Fig. 1. It can be noticed that the tree topology adopted reflects the schematic structure of an hexapod: the legs on the right and left side are connected to a central chain that we call backbone. This nine neuron structure has been considered more efficient than the minimal network, consisting of six neurons, since the backbone chain permits to have more robustness in presence of faults in the outer neurons, and also allows for the use of feedback signals which could be added for other types of locomotion control, like steering.

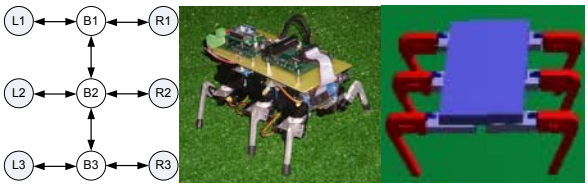

a) b) c)

Fig. 2. a) the MInihex structure; a)Network topology: the legs neurons (L1, L2,L3,R1,R2,R3) are connected with the backbone chain (B1,B2 and B3); b) the Minihex and c) its model in the dynamic simulation environment

To evaluate the minimum k value that guarantees the global synchronization to any chosen gait, we need simply to calculate the maximum Jacobian eigenvalue and the algebraic connectivity of the graph λ_1. It results: λ_{max} = 0.646, λ_1=0.2679 and then k_{min}=2.4110.

In the next Section, the results obtained using the constant k_{min} value for three different gaits, slow, medium and fast, are discussed.

Simulation were performed using a dynamic simulation environment based on the Open Dynamic Engine platform (Smith., 2010). The structure realised consists of a 12 degrees of freedom hexapod robot (Fig 2c), whose physical parameters strictly resemble the Minihex, an hexapod robot used for the experimental campaign (Fig 2b).

[1] The term "undirected" means that for each connection from the i node to j node, the same connection is duplicated in the opposite direction, from j to i.

In particular, the signals generated by the outer neurons of the network in Fig.2a are used to set the position values of the 12 servomotors used as the robot leg actuators. When suitable feedback control signals will be applied, the dynamic simulator can provide the feedback information of the trajectory really followed by the robot.

4.1 Convergence to specific gaits

For the topology depicted in Fig.2a, simulation results were obtained with the parameters reported in the previous Section. Since the k_{min} value assures the convergence to the synchronization subspace for any imposed gait, we have simulated the dynamics of the coupled system choosing k=2.5 in Eq.(5). For the nine-neuron topology of Fig.2a, the phase shifts defining the rotational matrices for the selected gaits are shown in Table 1. The nodes in the backbone are imposed to be synchronized in phase. The results obtained are shown in Fig.3. In the upper side, the stepping diagrams, showing the migration among the three considered gaits, are depicted. In the bottom side of Fig.3 the waveforms corresponding the six outer neurons of Fig.2a are reported. The L matrix parameters are switched at defined time instants and the convergence toward the new phase regime after a limited transient can be appreciated.

The same strategy has been used to control the Minihex, using a position control for the twelve actuators, as mentioned above when dealing with the dynamic simulator. A video depicting the robot motion is reported in the web page (Arena *et all*., 2010a).

5. TURNING STRATEGIES

A main interest regards the possibility of introducing strategies for an efficient turning of the robot. The approaches herewith proposed are mainly open loop methods. In fact here the interest lies in the possibility of finding key parameters useful for an efficient control. These ones will be used to subsequently close the loop with the environment.

For example, in walking flies, steering is achieved by concurrent changes in the step length and stepping frequency. In the legs on the outside of a curve to be faced with, the step length depends on the stepping frequency, just like during straight walking; turning is achieved by decreasing the step lengths on the inner side (Wannek et al., 1997).

Starting from the results obtained in the previous Sections, specific parameters within the CPG network can be identified in order to create a dissymmetry between the amplitudes of the cells used to control the two groups of ipsilateral legs. This will result in a modulation of the step length, as prescribed by the biological observation. In the following, simulation results are derived, which are currently under a deep study in order to be theoretically addressed.

Table 1. Phase displacements of each leg with respect to the backbone chain for specific gaits.

Gait	$\Delta\phi_{L1,B1}$	$\Delta\phi_{R2,B2}$	$\Delta\phi_{L3,B3}$	$\Delta\phi_{R1,B1}$	$\Delta\phi_{L2,B2}$	$\Delta\phi_{R3,B3}$
Slow	0°	60°	120°	180°	240°	360°
Med.	0°	90°	180°	180°	270°	360
Fast	0°	0°	0°	180°	180°	180°

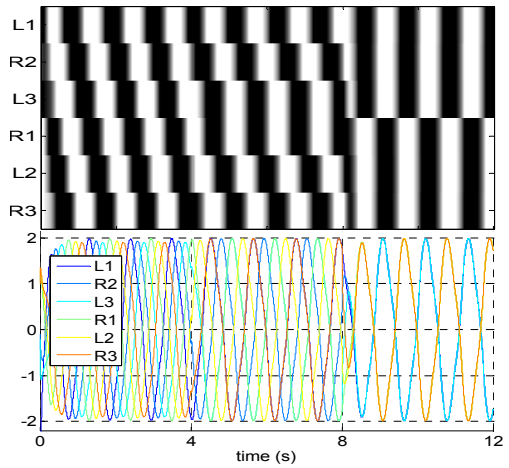

Fig. 3. Locomotion pattern (top) and the waveforms (bottom) for the six limbs of the hexapod migrating toward different gaits. The pattern is changed every 4s, migrating from the slow to the medium and to the fast gait. The connection matrix is updated from table 1.

5.1 Steering control based on frequency gain

A candidate parameter for steering control is the frequency gain γ that can be applied to specific cells to modify their dynamics. This parameter was already applied for gait control obtaining a smooth transition between different locomotion patterns (Arena *et all*., 2010a). When γ of ipsilateral legs is modified, the oscillation frequency of the uncoupled system changes accordingly and through the diffusive connections the network finds a new equilibrium condition. If γ is applied only to the reactive part $f(.)$ in eq.(2), this becomes:

$$x_i = \gamma_i f(x_i, t) + k \sum_{j \neq i;\, j \in N_\eta} (R_{ij} x_j - x_i) \qquad (6)$$

In the case of two neurons, (Seo *et all*., 2007), imposing the equilibrium on the modules and the matching between the angular velocities in the polar representation of the dynamics of two cells, the existence of stable solutions for the phase can be easily proven, involving also an amplitude difference at the equilibrium. The results here reported are numerically extended to the network of Fig.2a, but further mathematical proof is currently under investigation. The results are shown using the ODE dynamic environment. Fig.4a-b show the steady state behavior of the outer neurons before and after the steering control application. The simulated robot starts moving straight in the North-South direction, (y axis in Fig.4c) with a slow gait and γ=1; after t=5.4s, γ=6 is applied to the left side legs. This causes a reduction in the step length on the contralateral side (Fig.4). As the frequency of one side is increased, the signal amplitude of the contralateral legs decreases and a new frequency and phase equilibrium is also achieved. This side aspect depends on coupling of dynamics with different frequencies. It was also experimentally observed that γ>1 causes a phase lead on the stimulated legs (L1, L2 and L3 in Fig 4.b). Moreover, the additive phase shift affects the locomotion only during the steering time since the dynamics comes back to the pre-existing pattern when the steering control is stopped. Due to the lead effect on the phase of the stimulated legs, the gait pattern undergoes a

phase drift from the slow to a new steady state condition which is a "quasi-fast" locomotion pattern. Notably, a smooth modulation of γ causes a smooth change in the amplitude difference between the contralateral control signals and a smooth phase drift, which are necessary conditions for a smooth steering control.

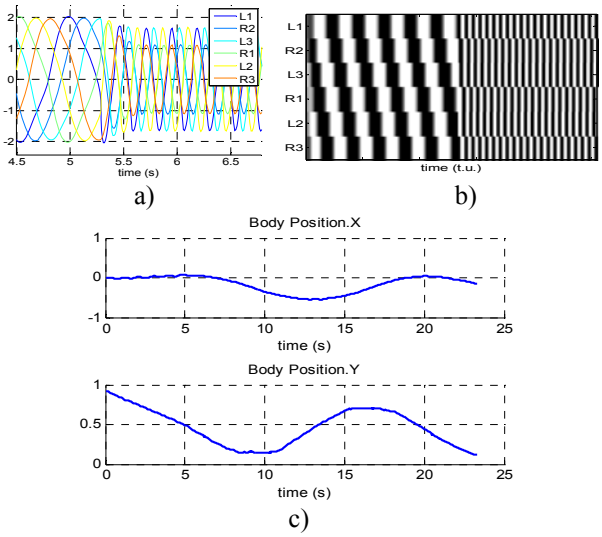

Fig. 4. Waveforms (a), stepping diagram (b) and body position (c) when γ=6 is applied on the L1,L2,L3 legs at 5.4s starting from the slow gait. The amplitudes in the opposite side decrease (a), the phase leads on the left side (b) and turning on the right takes place (c).

5.2 Steering control based on the coupling weights

Another approach for steering control is the introduction of a different coupling gain in the diffusive connections among particular neurons. Eq.(2) is thus rewritten as:

$$x_i = f(x_i, t) + k \sum_{j \neq i; j \in N_{r_1}} (R_{ij}(w_{ij} x_j) - x_i) \qquad (7)$$

where w_{ij} <1 are used in the connections of the neurons belonging to the same side as the turning direction. In fact, when the coupling gain w_{ij} is unique for the whole network, the phase convergence is reached, retaining also the same amplitude as the uncoupled cells. Using space variant weights, the steady state amplitude is no longer the same. It was also found that the weight modulation has no effect on the pre-existing phase equilibrium: so the imposed gait is preserved. On the other side the frequency changes, although the effect is lighter than applying the frequency gain-based strategy. In Fig. 5 the waveforms for the outer neurons and the locomotion pattern during the steering period for the slow gait are reported. The phase shifts among the neurons are defined as in Table 1. The value w_{ij}=0.5 was selected for the connections linking the L1, L2, L3 limbs to the backbone, and w_{ij} =1.5 for connection on the opposite side, including the links along the backbone. Similar results are obtained with the other two gaits (medium and fast). The-steering behavior obtained adopting this strategy on the dynamic simulation environment is depicted in Fig. 6. Notably, unlike the case of the steering control with frequency gain, the locomotion pattern is not affected by any additive phase error. Moreover, the new steady state frequency is very near to the one of the uncoupled oscillators.

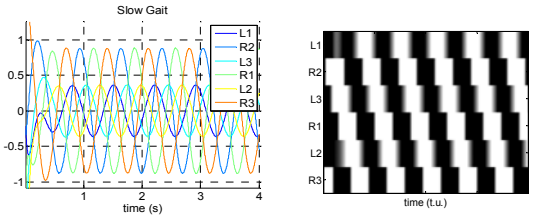

Fig. 5. Steering control based on the coupling weights The left figure shows the lower amplitudes in the signals having w<1; the right one shows that the stepping diagram is retained during steering.

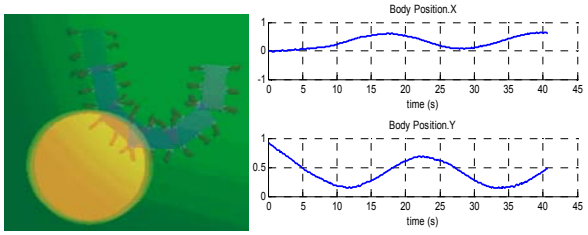

Fig. 6. Right, the overlap of a set of frames extracted every 4 s after the steering control is applied. Left, the corresponding x and y trajectories of the robot body.

6. REMARKS AND CONCLUSIONS

In this paper the stability of a CPG network, based on dynamical systems and adopted for the locomotion control of a hexapod robot is analyzed using the partial contraction theory. In particular, for the adopted tree graph network structure, analytical conditions for a unique gain value are derived to control the hexapod walking for any chosen locomotion gait. These results are also supported by simulations and experimental validations on a hexapod robot with 12 dof. Furthermore specific parameters have been identified for the introduction of turning strategies inspired by insect experiments. In this case, extensive simulation results on a dynamic simulation environment support the strategies introduced. It is to be outlined that in this paper an open loop approach to the analysis of CPG schemes was adopted for two reasons: the first was to find analytical conditions on the migration among different locomotion patterns, and the second, related to the steering control, was to identify the key control parameters, which can subsequently be used to close the loop with the environment. The simplest strategy can make use of visual signals to detect the presence of obstacles that can induce a modulation of the frequency gain or of the connection values to implement the turning behaviour. Other strategies could exploit inputs from collision sensors placed on the legs to locally modulate the dynamics of the corresponding neuron. However in this case the stability condition should be accurately checked, since the eigenvalues of the Jacobian matrix change.

Effort is being currently paid in order to analytically formalize this approach. Finally, the CPG model structure studied, using the piecewise linear approximation of the cell nonlinearity, was already realized and implemented by the authors using a Cellular Nonlinear network approach and also some VLSI prototypes were devised. This allows for a more efficient use of the available hardware, taking into account the analytical conditions here formalized.

ACKNOWLEDGMENT

The work was supported by the E.C. project ICT 216227 - SPARK II and ICT 270182 - EMICAB.

REFERENCES

Arena, P. Fortuna L., Frasca, M. Patané, (2005) L. "A CNN-based chip for robot locomotion control", IEEE Trans. *Circuits and Systems I:*Vol.52, 9, pp:1862 – 1871

Arena P., Patanè (2010a) L. SPARK II Project Multimedia: www.spark2.diees.unict.it/HexapodalControl.html

Arena E., Arena P. Patanè L., (2010b) Frequency-driven gait control in a Central Pattern Generator, Int. Conf. on Appl. Bionics and Biomecanics (ICABB), Venice Italy.

Beer, R. D. Chiel, H. J. Quinn, R. D. Espenschied, K. S.and Larsson, P. (1992)"A distributed neural network architecture for hexapod robot locomotion," *Neural Computat.*, no. 4, pp. 356–365.

Collins J. J. and Stewart, I. N. (1993) "Coupled nonlinear oscillators and the symmetries of animal gaits," *J. Nonlinear Sci.*, pp. 349–392.

Fiedler M (1973)., Algebraic connectivity of graphs, Czech. Math. Journal 23, 298-305.

Frasca, M. Arena, P. Fortuna, L .(2004) *Bio-inspired emergent control of locomotion systems*, World Scientific Serie A, vol. 48.

Fukuoka, Y. Kimura, H. and A. H. Cohen, (2003) "Adaptive dynamic walking of a quadruped robot on irregular terrain based on biological concepts," *Int. J. Robot. Res.*, vol. 22, no. 3–4, pp. 187–202.

Golubtisky, M. Stewart, I. Buono, P. and Collins, J. J. (1998) "A modular network for legged locomotion," *Physica. D*, vol. 115, pp. 56–72.

Klaassen B., Linnemann, D. Spenneberg, F. Kirchner, "Biomimetic walking robot scorpion: Control and modeling," *Robot. Auton. Syst.,* vol. 41, no. 2–3, 2002.

Lewis, M. A. Etienne-Cummings, R. Cohen, A. H. and M. Hartmann, (1998) "Toward biomorphic control using custom avlsi cpg chips," in *Proc. Int. Conf. Robotics and Automation*, San Francisco, CA.

Lohmiller W. and Slotine J.J., (1996)On Metric Observers for Nonlinear Systems *Proc. IEEE Int. Conference on Control Applications* Dearborn, MI.

Orlovsky, G. N. Deliagina T. G., and Grillner, S. (1999) *Neural Control of Locomotion.* Oxford Press**.**

Pham Q.C., Slotine, J.J. (2007), Stable concurrent synchronization in dynamic system networks, Neural Networks 20 (2007) 62–77.

Quinn R. D.and. Ritzmann, R. E (1998) "Construction of a hexapod robot with cockroach kinematics benefits both robotics and biology," *Connect. Sci.*, vol. 10, no. 3–4,.

Seo K.and Slotine, J. E. (2007) Models for Global Synchronization in CPG-based Locomotion, *IEEE Int. Conference on Robotics and Automation*, Roma, Italy.

Smith R. (2010), Open Dynamics Engine: www.ode.org.

Wang, W., & Slotine, J. -J. (2005), On partial contraction analysis for coupled nonlinear oscillators, Biol. Cybernetics, 92(1), 38–53

Wannek U, Strauss R (1997) Turning strategies in the walking fly, Drosophila melanogaster. Journal of Neurogenetics 11:207-208

Zielinska T. and Heng, J. (2002) "Development of a walking machine: Mechanical design and control problems," Mechatronics, vol. 12, pp. 737–754.

Appendix A

Below we report a proof of the result reported in eq.(5).

When global synchronization (i.e. null phase among the oscillators) is requested, the coupling matrix L matches the classical Laplacian matrix of the graph and M_r is defined as: $M_r = \{R(0)\, x_j = x_i \ \forall\ i,j\}$ with $r = 1,..,p$.

To define the global flow invariant subspace M, note that in the case of a tree graph, all rotational constraints among the units can coexist within a unique synchronization group[2] leading to have $p=1$ and:

$$M = \left(\left[R(0) \quad R(0) \quad \cdots \quad R(0)\right]\right)^T \in R^{n_t \times n_c} \qquad (8)$$

Consequently it results:

$V \in R^{n_t \times (n_t - n_c)}$ and $V^T L V \in R^{(n_t - n_c)\times(n_t - n_c)}$.

Since the network is connected and being L positive semidefinite, the eigenvalues of L are $0=\lambda_0 < \lambda_1 \le \lambda_2 \le \ldots \le \lambda_{n-1}$ each one with multiplicity equal to n_c. Moreover it results $\lambda_0 = 0$ and λ_1 is the so-called algebraic multiplicity of the graph. At this point the result is a natural consequence of the following facts:

1. From M built as in eq. (8) it derives that: $LM = 0$ and M is the subspace of the eigenvectors associated with λ_0 .

2. The calculation of the following similarity transformation, yields to:

$$\left[M \mid V\right]^{-1} L \left[M \mid V\right] = \left[M \mid V\right]^T L \left[M \mid V\right] = \begin{bmatrix} O & O \\ O & V^T L V \end{bmatrix}$$

It results that all the nonvanishing eigenspectrum of L is contained in $V^T L V$, and therefore $\lambda_{\min}(V^T L V) = \lambda_1$.

It is to be noticed that point 1 does not depend on the particular definition of M, e.g. on the particular choice of the flow-invariant subspace M, since for any given phase shift among the oscillators imposed through the L matrix, if M is of minimal dimensions it always results $LM=0$. Also point 2 is satisfied consequently.

Since the eigenspectrum of L and in particular λ_1 does not depend of the particular phase shift imposed, eq.(5) provides a unique sufficient condition on the gain value K able to control the trajectories toward any specified flow-invariant subspace, i.e. λ_1 depends only on the network topology and can be calculated a priori. Also $\sup_{x_i,t} \lambda_{\max}\left(\frac{\partial f}{\partial x}(x_i,t)\right)$ is calculated considering the uncoupled dynamics, preliminary chosen in the network.

Remark: in case M is chosen of dimensions larger than n_c, it results: $\lambda_{\min}(V^T L V) > \lambda_1$ and therefore eq.(5) is *a fortiori* satisfied selecting K in correspondence of λ_1.

[2] For more complex topologies, with cyclic paths, to define the total set of rotational constraints between each couple of nodes, the network needs to be partitioned in p synchronization groups and p Mr matrices must be defined.